

AD _____

GRANT NUMBER DAMD17-94-J-4120

TITLE: Ret Receptor: Functional Consequences of Oncogenic
Rearrangements

PRINCIPAL INVESTIGATOR: Susan S. Taylor, Ph.D.

CONTRACTING ORGANIZATION: University of California, San Diego
La Jolla, California 92093-0934

REPORT DATE: October 1997

TYPE OF REPORT: Annual

PREPARED FOR: Commander
U.S. Army Medical Research and Materiel Command
Fort Detrick, Frederick, Maryland 21702-5012

DISTRIBUTION STATEMENT: Approved for public release;
distribution unlimited

The views, opinions and/or findings contained in this report are those of the author(s) and should not be construed as an official Department of the Army position, policy or decision unless so designated by other documentation.

19980408 059

DTIC QUALITY INSPECTED 2

REPORT DOCUMENTATION PAGE

Form Approved
OMB No. 0704-0188

Public reporting burden for this collection of information is estimated to average 1 hour per response, including the time for reviewing instructions, searching existing data sources, gathering and maintaining the data needed, and completing and reviewing the collection of information. Send comments regarding this burden estimate or any other aspect of this collection of information, including suggestions for reducing this burden, to Washington Headquarters Services, Directorate for Information Operations and Reports, 1215 Jefferson Davis Highway, Suite 1204, Arlington, VA 22202-4302, and to the Office of Management and Budget, Paperwork Reduction Project (0704-0188), Washington, DC 20503.

1. AGENCY USE ONLY (Leave blank)		2. REPORT DATE October 1997	3. REPORT TYPE AND DATES COVERED Annual (15 Sep 94 - 14 Sep 97)	
4. TITLE AND SUBTITLE Ret Receptor: Functional Consequences of Oncogenic Rearrangements			5. FUNDING NUMBERS DAMD17-94-J-4120	
6. AUTHOR(S) Susan S. Taylor, Ph.D.				
7. PERFORMING ORGANIZATION NAME(S) AND ADDRESS(ES) University of California, San Diego La Jolla, California 92093-0934			8. PERFORMING ORGANIZATION REPORT NUMBER	
9. SPONSORING/MONITORING AGENCY NAME(S) AND ADDRESS(ES) Commander U.S. Army Medical Research and Materiel Command Fort Detrick, Frederick, Maryland 21702-5012			10. SPONSORING/MONITORING AGENCY REPORT NUMBER	
11. SUPPLEMENTARY NOTES				
12a. DISTRIBUTION / AVAILABILITY STATEMENT Approved for public release; distribution unlimited			12b. DISTRIBUTION CODE	
13. ABSTRACT (Maximum 200) Ret/ptc2 is a soluble, constitutively active oncogenic protein whose gene was cloned from human papillary thyroid carcinomas. Ret/ptc2 is a chimeric protein resulting from a reciprocal chromosomal rearrangement translocation event between the cAMP-dependent protein kinase regulatory subunit type I α (RI α) and the tyrosine kinase domain of the Ret receptor. Earlier microinjection studies showed the RI α dimerization domain is critical for eliciting a mitogenic response in mouse 10T1/2 fibroblasts. By combining results obtained from microinjection studies of Ret/ptc2 point mutants and mapping proteins identified from a yeast two-hybrid screen to a computer-generated model of the Ret/ptc2 kinase core, we have previously identified specific tyrosine residues to which the SH2 domains of Grb10 and PLC γ , the second C-terminal LIM domain of Enigma, and the PTB domain of Shc interact. From our recent characterization of the Enigma-Shc dual association with Ret/ptc2 in mouse 10T1/2 fibroblasts, we propose the mitogenic response elicited by Ret/ptc2 requires Enigma for proper cellular localization and utilizes the Ras pathway via the recruitment and phosphorylation of Shc. In addition to these studies, we have overexpressed and purified His ₆ -Ret/ptc2 from the methylotrophic yeast, <i>Pichia pastoris</i> , to initiate extensive <i>in vitro</i> biochemical and biophysical characterization.				
14. SUBJECT TERMS Breast Cancer <i>Pichia pastoris</i>			15. NUMBER OF PAGES 27	
17. SECURITY CLASSIFICATION OF REPORT Unclassified			16. PRICE CODE	
18. SECURITY CLASSIFICATION OF THIS PAGE Unclassified		19. SECURITY CLASSIFICATION OF ABSTRACT Unclassified		20. LIMITATION OF ABSTRACT Unlimited

FOREWORD

Opinions, interpretations, conclusions and recommendations are those of the author and are not necessarily endorsed by the U.S. Army.

X Where copyrighted material is quoted, permission has been obtained to use such material.

 Where material from documents designated for limited distribution is quoted, permission has been obtained to use the material.

X Citations of commercial organizations and trade names in this report do not constitute an official Department of Army endorsement or approval of the products or services of these organizations.


 In conducting research using animals, the investigator(s) adhered to the "Guide for the Care and Use of Laboratory Animals," prepared by the Committee on Care and Use of Laboratory Animals of the Institute of Laboratory Resources, National Research Council (NIH Publication No. 86-23, Revised 1985).

 For the protection of human subjects, the investigator(s) adhered to policies of applicable Federal Law 45 CFR 46.

X In conducting research utilizing recombinant DNA technology, the investigator(s) adhered to current guidelines promulgated by the National Institutes of Health.

X In the conduct of research utilizing recombinant DNA, the investigator(s) adhered to the NIH Guidelines for Research Involving Recombinant DNA Molecules.

X In the conduct of research involving hazardous organisms, the investigator(s) adhered to the CDC-NIH Guide for Biosafety in Microbiological and Biomedical Laboratories.


PI - Signature

Oct 12, 1997
Date

TABLE OF CONTENTS

	<u>Page</u>
(1) FRONT COVER	1
(2) SF 298, REPORT DOCUMENTATION PAGE	2
(3) FOREWORD	3
(4) TABLE OF CONTENTS	4
(5) INTRODUCTION	5
(6) BODY	8
(7) CONCLUSIONS	26
(8) REFERENCES	26

INTRODUCTION

Protein phosphorylation is probably the most important mechanism for regulation in eukaryotic cells. The tightly regulated enzymes that catalyze the phosphorylation of proteins, the protein kinases, are important components of signaling pathways that regulate normal cellular functions such as the cell cycle, metabolism, differentiation, memory and response to hormones, to name only a few. Over 400 are now known (1) and mutations that generate unregulated or constitutively activated protein kinases are typically oncogenic.

One of the simplest members of the protein kinase family is the cAMP-dependent protein kinase, cAPK (2). Being one of the best understood members of the protein kinase family, cAPK also serves as a template for the others since all of these enzymes have evolved from a common ancestor and contain a conserved catalytic core. cAPK, in the absence of cAMP, contains two types of subunits, a regulatory (R) subunit and a catalytic subunit (C). The R_2C_2 holoenzyme is catalytically inactive. In the presence of cAMP the complex dissociates into an R_2 -(cAMP) $_4$ dimer and 2 free and active C-subunits. The crystal structure of the C-subunit, solved in our laboratory, serves as a structural template for the entire family of protein kinases (3). It defines the folding of the polypeptide chain as well as the positions of the invariant residues that mostly cluster around the active site (4).

The objective of this grant is to characterize a novel oncogenic tyrosine kinase, Ret/ptc2, found in human papillary thyroid carcinomas. Specifically, we want to understand the molecular basis for its constitutive activation and the basis for its oncogenic properties. Ret/ptc2 is a rearranged gene product composed of the cAMP-dependent protein kinase (cAPK) regulatory subunit $I\alpha$ ($RI\alpha$) at its N-terminus fused to the tyrosine kinase core of a proto-oncogene, the Ret receptor (RetR).

Ret Receptor

RetR was cloned from a THP-1 human monocytic leukemia cDNA library, and is expressed in a number of human neuroblastoma and leukemia cell lines as 140-190 kDa glycoproteins (5). Sequence analysis identified it to be a member of the receptor tyrosine kinases, and *in situ* hybridization and mutations of the RetR gene show its function is important for enteric neurogenesis and kidney organogenesis in the mouse (6, 7, 8) and for normal development of motor and dopaminergic neurons (9). Activation of RetR requires the binding of glial-derived neurotrophic factor (GDNF), to a glycosylphosphatidylinositol linked receptor, GDNF α , and the association of this complex to RetR (9, 10, 11, 12). Homozygous knockout experiments of the GDNF gene result in both kidney agenesis and the absence of enteric innervation to the digestive system (13). Chromosomal rearrangements of human RetR with other genes and point mutations of RetR have been linked to a number of human cancers and Hirshprung's disease.

The Ret Oncogene Family

The family of Ret oncogenes can be divided into three separate classes. The first class was produced by transfecting NIH3T3 cells with high molecular weight DNA from human cell lymphomas (14) human colon carcinoma (15) and human stomach cancer tissue (16). The high propensity of *proto-ret* to rearrange with other genes is reflected in its name for *re*arranged upon *tr*ansfection (14).

The second class consists of missense mutations and truncated forms of RetR that are proposed to result in either hyper- or hypoactivity. These are associated with three dominantly inherited human cancer syndromes: MEN 2A (17) MEN 2B, familial medullary thyroid carcinoma (FMTC) (18, 19) and Hirschsprung's disease (20, 21).

The third class of Ret oncogenes, isolated from human papillary thyroid carcinomas (PTC) (22, 23, 24, 25) consists of 3 subtypes: *ret/ptc1*, *ret/ptc2* and *ret/ptc3*. The 5' end of the each oncogene is a portion of an unrelated gene fused in frame to the identical splice site of the RetR gene resulting in an intact and functional Ret tyrosine kinase.

The PTC-type oncogenes each encode 2 protein isoforms as a result of alternative splicing at the 3' end, and unlike RetR are completely cytosolic, phosphorylated on tyrosine residues, and constitutively active (24). The 5' end of *ret/ptc1* is a fragment of a new gene designated, H4(DS10S170) (23, 26) and the 5' end of *ret/ptc3* encodes a gene designated *ele1* or ret-fused gene, whose gene product does not show sequence identity to known proteins (24, 27, 28). Unlike *ret/ptc1* and *ret/ptc3*, the N-terminal sequence of *ret/ptc2* (24) encodes approximately 60% of a biochemically well characterized protein, the RI α subunit of cAPK. A comparison of RetR, Ret/*ptc2*, and the cAPK RI α -subunit is illustrated in Figure 1.

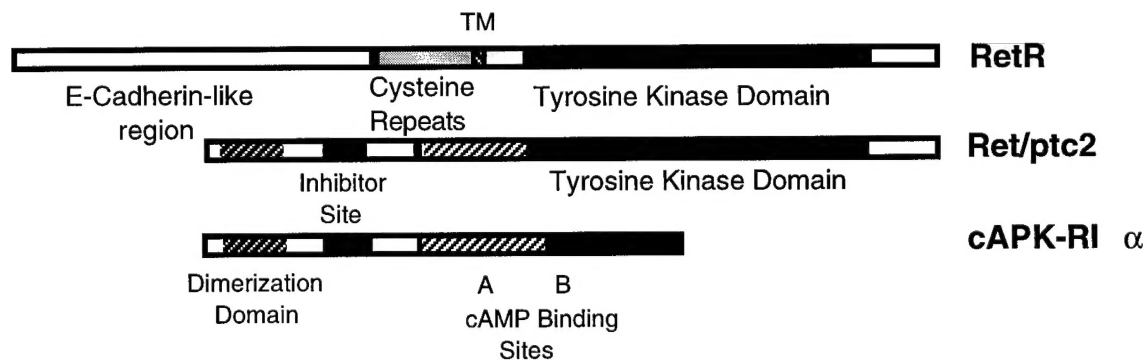


Figure 1. Comparison of RetR, Ret/*ptc2*, and the cAPK RI α subunit

Regulatory Subunit of cAPK

The regulatory subunit of cAPK maintains the C-subunit in an inactive state by forming a stable R₂C₂ tetramer. A pseudo-substrate inhibition sequence in the R-subunit mimics peptide substrates and fills the peptide binding site of the C-subunit. The binding of cAMP to the R-subunit causes the complex to dissociate and release two active C-subunits.

Although there are several unique gene products in the R-subunit family, all share a well-defined domain structure. The RI α subunit begins with a dimerization domain close to its amino terminus followed by a pseudo-substrate inhibitory region and ends with two tandem cAMP binding domains, A and B. The RI α dimerization domain is stabilized by two antiparallel interchain disulfide bonds (29). Circular dichroism studies of the proteolytically isolated RI α dimerization domain indicate it is predominantly α -helical, and extremely stable to thermal denaturation (30). The crystal structure of a deletion mutant of bovine RI α was recently solved in our laboratory (31). The splice site of the RI α fragment in Ret/ptc2 is at the beginning of the α C-A helix, thus deleting the last 21% of the A-site cAMP-binding domain and the entire B-site cAMP binding domain.

SPECIFIC AIMS

Our overall long-term goals are to understand the molecular basis for the constitutive activation of Ret/ptc2 and to characterize the physiological function of both Ret/ptc2 and RetR. Our specific aims are the following:

1. To model the kinase core of Ret/ptc2 based on the crystal structures of both the C-subunit of cAPK and the kinase domain of the insulin receptor.
2. To understand the structural features of Ret/ptc2 that are required for its oncogenic properties. To achieve this we have developed an *in vivo* assay to measure the mitogenic response of Ret/ptc2 by nuclear microinjection of *ret/ptc2* into mouse 10T1/2 fibroblasts.
3. To identify Ret/ptc2 associated proteins using a yeast two-hybrid screen.
4. To characterize the biochemical properties of Ret/ptc2 by overexpressing the protein in *E. coli* and human kidney 293 cells. Phosphorylation sites will be mapped and kinetic properties characterized.
5. To construct homologs of Ret/ptc2 using the tyrosine kinase domains of the EGF receptor and the insulin receptor.

We have made excellent progress in each of these areas during the past two and a half years as described in the last annual project report. In the past year, we have added to our understanding of Ret/ptc2 in two areas. We have continued to define how Ret/ptc2 signals in mitogenesis. In addition, we have utilized a yeast expression system to overexpress Ret/ptc2 in large quantities thus allowing us to initiate comprehensive biochemical and biophysical studies. We will concentrate on these two topics in this report in fair detail although some of the techniques described below are similar to those reported previously.

MATERIALS AND METHODS

A. Shc and Enigma Association with Ret/ptc2 Mitogenic Signaling

I. DNA Constructs

The mammalian expression plasmids coding for wild-type and mutants of Ret/ptc2 were constructed in pRc/CMV (Invitrogen) as described previously (32, 33). Construction of the hemagglutinin (HA)-tagged Enigma expression constructs was also described previously (34). Human Shc cDNA, kindly provided by David Schlaepfer (Scripps Institute, La Jolla, CA), was subcloned into pRSETb (Invitrogen), and NotI sites were introduced by site-directed mutagenesis (35) to allow excision of the sequence encoding either full-length Shc, the phosphotyrosine binding (PTB) domain (residues 1-213), or the Src homology 2 (SH2) domain (residues 373-479). These fragments were then subcloned into the NotI site of pGEX (Pharmacia), pcDNA3M (34) and pVP16. Plasmids expressing dominant-negative Ras (N17) and the N-terminal epitope (NTE) of Raf were obtained from Akhlesh Pandey (University of Michigan, Ann Arbor, MI). To create the C-terminal fusion of Ret/ptc2 with the Enigma PDZ domain (C'574-PDZ), Ret/ptc2 cDNA was subcloned into the HindIII and XbaI sites of pcDNA3 (Invitrogen), a linker was added at the XhoI site in the Ret/ptc2 sequence which created a unique EcoRI site, and then cDNA coding for the N-terminal 279 residues of Enigma was subcloned into the EcoRI and XhoI sites. The plasmid expressing PLC γ Shc was constructed by subcloning cDNA encoding residues 214-479 of Shc into pcDNA3M, and then splicing a PCR-generated fragment of PLC γ 2 in between the HA-tag and the Shc sequences. This fragment of PLC γ 2 encodes the N-terminal SH2 domain which was previously demonstrated to bind Ret/ptc2 (33).

II. Cell Culture and Microinjection

Mouse 10T1/2 fibroblasts were plated in Dulbecco's modified Eagle medium containing 10% fetal bovine serum (DMEM + 10% FBS). The cells were maintained at 37°C in a 10% CO₂ atmosphere and split before reaching confluence. For microinjection, cells were plated on glass cover slips and grown to 70% confluence in DMEM + 10% FBS. The cover slips were then transferred to starvation medium (DMEM containing 0.05% calf serum). After incubation for twenty-four hours in the starvation medium, the cells were injected into their nuclei with injection buffer (20 mM Tris pH 7.2, 2 mM MgCl₂, 0.1 mM EDTA, 20 mM NaCl) containing 100 µg/ml of each expression plasmid DNA and 6 mg/ml of either guinea pig or rabbit IgG (Sigma). All microinjection experiments were performed using an automatic micromanipulator (Eppendorf, Fremont, CA), with glass needles pulled on a vertical pipette puller (Kopf, Tujunga, CA).

III. Mitogenic Response Assay

DNA synthesis was assessed through incorporation of the thymidine analog 5-bromodeoxyuridine (BrdU) and its subsequent detection by immunostaining. Following nuclear microinjection, 0.1% BrdU labeling reagent (Amersham) was added to the starvation medium, and the cells were incubated

for an additional 24 hours. Cells were fixed in 95% ethanol/5% acetic acid for thirty minutes, and then washed with phosphate buffered saline (PBS). Incorporation of BrdU was visualized by successively incubating the fixed cells with mouse anti-BrdU (undiluted), biotinylated donkey anti-mouse IgG (dilution 1:500), Texas Red streptavidin (dilution 1:100), and FITC anti-Rabbit IgG (dilution 1:100). Cells were scored by fluorescent microscopy for nuclear microinjection (FITC positive) and BrdU incorporation (Texas Red positive).

IV. Detection of Expressed Protein by Immunofluorescence

For observation of expressed protein, cells were fixed five hours post-injection in 3.7% formaldehyde for five minutes, and then washed with PBS and incubated with blocking buffer (2% goat serum, 2% BSA, 0.1% Triton X-100, 50 mM glycine, in PBS) for twenty minutes. For detection of Ret/ptc2, cells were then incubated successively with rabbit anti-Ret (dilution 1:500), biotinylated donkey anti-rabbit IgG (dilution 1:400), Texas Red streptavidin (dilution 1:100), and FITC anti-guinea pig IgG (dilution 1:100). For detection of HA-tagged Enigma constructs, the same procedure was followed except the first two antibodies were replaced with mouse monoclonal anti-HA antibody (dilution 1:250) followed by biotinylated donkey anti-mouse IgG (dilution 1:400). The co-injected samples examined by confocal microscopy were fixed in the same manner, and incubated with the following antibodies: rabbit anti-Ret (1:500), biotinylated donkey anti-rabbit IgG (1:400), Cy-5 streptavidin (1:100), mouse monoclonal anti-HA antibody (1:250), donkey FITC anti-mouse (1:250), and AMCA donkey anti-guinea pig IgG (1:100). Confocal images were collected on an MRC-1024 system (Bio-Rad) attached to an Axiovert 35M (Zeiss AG), with excitation illumination from a krypton/argon laser. Individual images (1024 x 1024 pixels) were converted to PICT format and merged as pseudo-color red/green/blue images using Adobe Photoshop (Adobe Systems). Digital prints were produced with a Fujix Pictography 3000 printer.

V. Yeast Two-Hybrid Detection of Protein-Protein Interactions

A yeast two-hybrid system was used to screen for protein-protein interactions (36). Ret/ptc2 cDNA was subcloned into the LexA-fusion vector pBTM116 (bait), and point mutants were made by site-directed mutagenesis (35). Human Shc cDNA or PCR generated fragments were subcloned into pVP16 (prey). These constructs were co-expressed in the L40 strain of *S. cerevisiae*, and single colonies were either plated on solid media containing 100 µg/ml X-gal or added to 5 ml liquid cultures an *in vitro* assay measuring β-galactosidase activity (37). Aliquots from these cultures were used to seed fresh cultures which were grown to an OD₆₀₀ of approximately 0.5. Cell pellets from a 5 ml culture were resuspended in 0.5 ml of Z buffer (60 mM Na₂HPO₄, 40 mM NaH₂PO₄, 10 mM KCl, 1 mM MgSO₄, 50 mM β-mercaptoethanol, pH 7.0). Samples of these resuspensions were diluted 10 to 40-fold (final volume 1 ml) in Z buffer. Cells were lysed by addition of sodium dodecylsulfate (SDS) and chloroform followed by vortexing. The chromagenic substrate o-nitrophenyl-β-D-galactoside was added (200 µl of 4 mg/ml solution), and the reaction was quenched by addition of 0.5 ml of 1 M Na₂CO₃. Units of activity are calculated as: Activity = 1750(OD₄₂₀) / [(time in min)(volume of culture in assay)(OD₆₀₀ of culture)].

VI. GST-fusion Affinity Precipitation

Two-hybrid results were verified in a stably transfected NIH3T3 cell line expressing an epidermal growth factor receptor (EGFR)/Ret chimeric protein (38). These cells were treated with 100 nM EGF for 10 minutes before resuspension in lysis buffer (50 mM HEPES pH 7.4, 150 mM NaCl, 5 mM KCl, 1 mM CaCl₂, 1 mM MgSO₄, 10% glycerol, 1% Triton X-100, 1 mM benzamidine, 1 mM TPCK, 1 mM TLCK, 1 mM PMSF, 1 mM NaVO₄). Cleared lysates were incubated for 2 hours with approximately 5 mg of GST fusion protein bound to glutathione agarose beads (Sigma) in a total volume of 300 μ l. The beads were washed four times with lysis buffer, resuspended in laemmli loading buffer (39), and electrophoresed in a 7.5% sodium dodecylsulfate (SDS) polyacrylamide gel. Proteins were transferred to polyvinylidene fluoride (PVDF) membranes and blots were probed with either rabbit anti-Ret (1:25,000) or monoclonal anti-phosphotyrosine antibodies (1:2500, Transduction Laboratories). The GST-fusion proteins used were expressed in *E. coli* from pGEX vectors containing inserts coding for the following sequences: GST-empty vector; GST-ShcSH2 - human Shc SH2 domain, residues 373-479; GST-ShcPTB - human Shc PTB domain, residues 1-213; GST-Enigma- human Enigma LIM domains 2 and 3, the C-terminal 131 residues.

B. Expression and Purification of Ret/ptc2 in *Pichia pastoris* GS115

I. Subcloning *ret/ptc2* into pPICZb

The Ret/ptc2 gene was subcloned into the 3.3 kb pPICZb vector (Invitrogen) behind the alcohol oxidase promoter between the PmlI and NotI sites. The final construct, *ret/ptc2*/pPICZb, contains the first Met codon within the Kozak sequence, ACCATGG (40, 41) and encodes a c-Myc epitope at its C-terminus followed by a sextahistidine (His₆) tag. Competent TOP10F⁺ (Invitrogen) cells were transformed using the manufacturer's protocol and zeocin (25 mg/l) resistant colonies were grown for plasmid isolation. Plasmids were prepared using the Qiagen midi-prep kit and evaluated by both restriction digestion and double-stranded sequencing.

II. Transformation and Expression of Ret/ptc2 in *Pichia pastoris* GS115

ret/ptc2/pPICZB was linearized by restriction digestion with PmeI and the linearized construct was used to transform spheroplast wild-type *Pichia pastoris* GS115 cells according to the manufacturer's protocol (Invitrogen Pichia Expression Kit, v. C). Transformed cells were plated onto regeneration dextrose medium agarose plates (1 M sorbitol, 1 % dextrose, 1.34% yeast nitrogen base, 4 x 10⁻⁵% biotin, 0.005% amino acids, 0.004% histidine). Single colonies were picked to grow in yeast extract peptone dextrose medium (1% yeast extract, 2% peptone, 2% dextrose) at pH 4 to evaluate the level of His₆-Ret/ptc2 expression by SDS-polyacrylamide gel electrophoresis (PAGE) and Western analysis using anti-Ret polyclonal antibodies at 1:200000. Colonies producing the highest levels of His₆-Ret/ptc2 were inoculated in a 7 l Applikon fermentor containing 3.5 l fermentor basal salts, PTM1 basal salts (2 ml/l), and 4% glycerol. After 23 hours and complete glycerol depletion, the cell density was determined to be 106 grams/l wet cell weight. A 50% (w/v) glycerol + 1.2% (v/v) PTM1 feed was delivered at a

flow rate of 53 ml/hr and continued for 4 hours for a total volume of 210 ml glycerol. Cells were induced at a density of 137 g/l by delivering 100% methanol + 1.2% PTM1 at approximately 8 ml/hr for 4 hours, 16 ml/hr for 26 hrs, and 32 ml/hr for 48 hrs, for a total induction time of 74 hours and a total delivered methanol volume of 1950 ml. Feed delivery rates were maintained with a peristaltic pump, and the pH of the media was maintained at 4.0 throughout by the addition of NH₄OH. The final cell density was 413 grams/liter wet cell weight. The cells were harvested by centrifugation, and cell pellets were stored at -80 °C.

III. Purification of Ret/ptc2

Six grams of frozen cells from the fermentor preps were thawed and rinsed briefly in the following ice-cold buffer: 50 mM Tris-Cl, pH 8, 150 mM NaCl, 10 % glycerol. Cells were pelleted by centrifugation at 3000 x g for 10 minutes at 4 °C and lysed 8x for 30 seconds each in an equivalent amount of 425-600 µm acid-washed glass beads (Sigma) using both a beadbeater and a vortex at 4 °C followed by cooling on ice in the lysis buffer: 50 mM Tris-Cl, pH 8.0, 150 mM NaCl, 5 mM β-mercaptoethanol, 10 % glycerol, 2 mg/ml leupeptin, 100 mg/ml TPCK, 50 mg/ml TLCK, 0.1 mM 1,10-o-phenanthroline, 0.1mM PMSF and 0.1 mM 4-(2-aminoethyl)-benzenesulfonyl fluoride-HCl (AEBSF, Sigma). Cell lysates were centrifuged at 14000 x g for 10 minutes at 4 °C and the supernatant fraction, S1, was batch-bound to 0.8 ml cobalt resin (Clontech) at 4 °C for 30 minutes and His₆-Ret/ptc2 was batch-eluted from the resin 2x for 10 minutes each with 10 mls lysis buffer containing 10 mM imidazole at pH 7.9, 4 °C. Elutions were pooled and dialyzed (Spectra/Por 12-14,000 MW cutoff) against 2 l of 20 mM Tris-Cl, pH 8, 100 mM NaCl, 5 mM β-mercaptoethanol, 5% glycerol with 3 changes for at least 18 hours at 4 °C. Following dialysis, the dialysate was centrifuged in the Clinical centrifuge at maximum xg for 10 minutes at 4 °C, and filtered through a 0.8 µm/0.2 µm Acrodisc PF syringe filter (Gelman). His₆-Ret/ptc2 was purified using a BioLogic system (Bio-Rad) from an Uno-Q anion exchange column (Bio-Rad) in a linear gradient of 1.1 % NaCl/min in 20 mM Tris-Cl, pH 8, 5 mM β-mercaptoethanol, 5% glycerol. Peak fractions were determined by SDS-polyacrylamide gel electrophoresis (PAGE), peak fractions pooled, and concentrated at 4 °C in a stirred cell concentrator through a PM30 membrane (Amicon). During the concentration step, the buffer was exchanged to 50 mM HEPES, pH 8, 200 mM NaCl, 5 mM β-mercaptoethanol and 5% glycerol. Protein concentrations were determined with the Pierce Micro BCA kit following the manufacturer's protocol.

IV. Autophosphorylation Assay

Six microliters of purified His₆-Ret/ptc2 was added to 6 µl of a kinase mix containing 50 mM HEPES, pH 8, 150 mM NaCl, 10 mM MnCl₂, 100 µM dATP and [³²P]-dATP and incubated at room temperature for 10 minutes. Reactions were quenched with the addition of 4x laemmli loading dye (39), boiled for 3 minutes, and electrophoresed in a 10% SDS-PAGE gel. Following electrophoresis, the gel was stained in 1 g/l coomassie brilliant blue R-250 (Sigma) in 10% acetic acid and 25% isopropanol, destained in 10% acetic acid and 25% isopropanol, dried

between cellophane sheets in 10% ethanol, 5% glycerol at 37 °C, and exposed to K-OMAT-AR film (Kodak) at -80 °C between intensifying screens.

V. Native Polyacrylamide Gel Electrophoresis

A native mini acrylamide gel was prepared with 1.5 M Tris-Cl, pH 8.9, 7.62% acrylamide, 0.2% bis-acrylamide for the running gel and 0.5 M Tris-Cl, pH 6.8, 3.8% acrylamide, 0.1% bis-acrylamide for the stacking gel. Protein samples were diluted 1:1 with a 2x loading dye (0.12 M Tris-Cl, pH 6.8, 36% glycerol, bromophenol blue) and the gel run at 50 V in 0.025 M Tris-Base, 0.19 M glycine. Gels were stained as described above.

VI. Isoelectric Focusing

Ten to twenty micrograms of concentrated His₆-Ret/ptc2 and 20 µl of broad range isoelectric focusing standards (Pharmacia) were loaded onto a precast 5 % polyacrylamide gel and electrofocused at 7 °C at 3000 V for 1000 kV/hr using a Multiphor II electrophoresis unit (LKB). Gels were fixed in 0.7 M trichloroacetic acid, 0.136 M 5-sulphosalicylic acid for 45 minutes, rinsed well with de-ionized water, stained, and destained as described above.

VII. Molar Absorptivity Determination

Purified His₆-Ret/ptc2 was analyzed by Steve Smith in the laboratory of Jack Kyte, UC San Diego. The protein was spiked with norleucine and diluted 1:1 with 12 N HCl in a 5 ml glass vial (Wheaton). The vial was flushed for 2 minutes with argon gas, sealed and heated at 160 °C in 6N HCl for 50 minutes. The hydrolyzed protein was dried *in vacuo* over NaOH pellets and resuspended in 400 µl 0.2 N sodium citrate, pH 2.2, 0.5% thiodiglycol, 0.1% phenol. One eighth of the hydrolyzed protein was separated in a linear pH and salt gradient (Pickering Laboratories) in a modified HPLC equipped for cation-exchange chromatography, and post-column amino acids were derivatized with ninhydrin at 130 °C. Ninhydrin derivatives were detected with a dual wavelength HPLC detector at 570 nm for primary amines and 470 nm for secondary amines and analyzed by a printer/plotter integrator (Spectra Physics) for quantitation. The percent recovery of the protein was based on the percentage of norleucine recovered. The number of nmoles of each amino acid was determined by dividing the total number of nmoles recovered per amino acid by the integer number of each amino acid represented in the His₆-Ret/ptc2 primary sequence to determine the protein concentration. By measuring the absorption maxima of the protein solution and determining the concentration, the molar absorptivity was calculated using the Beer-Lambert Law.

VII. Equilibrium Analytical Ultracentrifugation

Purified His₆-Ret/ptc2 was loaded into a 6-hole, charcoal-filled Epon centerpiece fitted into a Beckman An60ti rotor and centrifuged at 3 speeds to equilibrium (approximately 20 hours per speed) in the Beckman model XL-I ultracentrifuge using the buffer: 50 mM HEPES, pH 8, 200 mM NaCl, 5 mM β-mercaptoethanol, 5% glycerol for the reference. Data sets for both absorbance at 280 nm and interference using Rayleigh interference optics were collected at each speed per hour and the approach to equilibrium was determined by calculating total RMS deviation of each data set from the last using the program MATCH

(Jeff Lary, National Analytical Ultracentrifuge Facility, Storrs CT). Equilibrium was determined empirically when no changes in RMS deviation between consecutive data sets were measured. Data was parsed from individual samples into separate data sets using the program REEDIT (Jeff Lary, National Analytical Ultracentrifuge Facility, Storrs CT).

RESULTS AND DISCUSSION

A. Shc and Enigma Association with Ret/ptc2 Mitogenic Signaling

Mitogenic signaling from Ret/ptc2 is blocked by dominant-negative forms of Ras and Raf

The mitogenic activity of Ret/ptc2 was measured using a microinjection assay in which serum-starved fibroblasts were injected with expression plasmids and subsequent entry into S-phase was assessed by incorporation of the thymidine analog 5-bromodeoxyuridine (BrdU) (32). Injection of a plasmid expressing Ret/ptc2 resulted in over 35% of the injected cells entering S-phase (Figure 2). In contrast, cells co-injected with the Ret/ptc2 construct and one expressing either a dominant negative form of Ras (N17) (42, 43) or Raf (NTE) (44) responded in a manner that was not significantly different from uninjected controls. The mitogenic activity of Ret/ptc2 thus requires the Ras pathway. Co-injection of a kinase-inactive form of *src* had no effect.

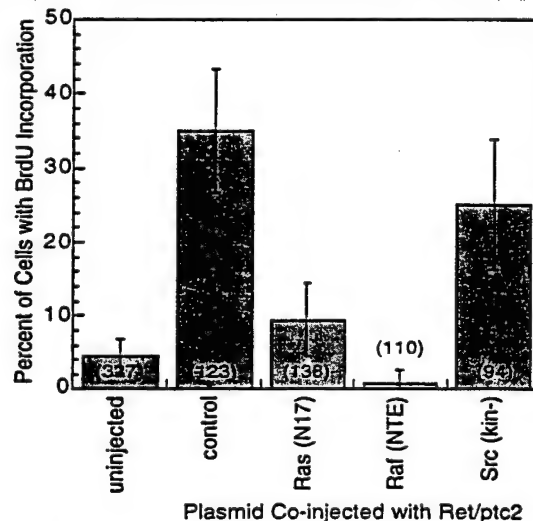


Figure 2. Serum-starved mouse 10T1/2 fibroblasts were microinjected with a mixture of the Ret/ptc2 expression plasmid with one of the following: a control empty plasmid (control), plasmid expressing serine 17 to asparagine mutant Ras [Ras(N17)], plasmid expressing N-Terminal Epitope, residues 1 through 290, of Raf-1 [Raf(NTE)], or plasmid expressing a catalytically inactive form of Src [Src(kin-)]. In each case, constructs were injected at 100 µg/ml. Cells were then assessed for entry into S-phase by immunofluorescent detection of BrdU incorporation. The fraction of injected cells positive for BrdU incorporation is shown with error bars displaying the 95% confidence interval calculated using the standard error of proportion. The numbers in parentheses are the total number of injected cells.

Co-localization of Ret/ptc2 and Enigma

Because activation of Ras requires recruitment of the guanine nucleotide exchange factor SOS to the plasma membrane (45, 46, 47), the sub-cellular distribution of Ret/ptc2 was investigated. Using immunofluorescent staining of cells injected with Ret/ptc2 expression constructs (Figure 3), Ret/ptc2 was found to have a distinctive pattern of localization where much of the cell periphery, including regions which resembled focal adhesions, stained most prominently, and filaments resembling the actin cytoskeleton were also visible (Figure 4A). This pattern was not present in cells expressing a form of Ret/ptc2 that lacked the C-terminal 22 residues, C'574, suggesting the C-terminus of Ret/ptc2 determines the localization of the protein to the plasma membrane (Figure 4B). A deletion mutant that eliminated the dimerization domain of Ret/ptc2, a region known to interact with A kinase anchoring proteins (AKAP's) (48) and to be required for mitogenic activity (32) did not affect the distribution of full-length Ret/ptc2 (Figure 4C). Localization is activity-independent, because kinase inactive forms of Ret/ptc2 also localized in a pattern indistinguishable from wild-type (data not shown).

A potential anchor for Ret/ptc2 is Enigma, a protein previously shown to interact with the C-terminus of Ret/ptc2 in an activity-independent manner (33, 34). To test this possibility, the distribution of Enigma was investigated by immunofluorescent staining. Because polyclonal antibodies raised against Enigma lacked the specificity required for this method, plasmids were injected which expressed HA-tagged forms of Enigma that could then be localized with anti-HA monoclonal antibodies (Figure 3). Full-length Enigma displayed a distribution pattern very similar to that of Ret/ptc2, with pronounced staining of the cell edges and some cytoskeletal components (Figure 4D). A deletion mutant of Enigma that lacked the PDZ domain exhibited a diffuse, cytoplasmic staining pattern (Figure 4E), while a mutant lacking all three LIM domains retained the wild-type distribution (Figure 4F).

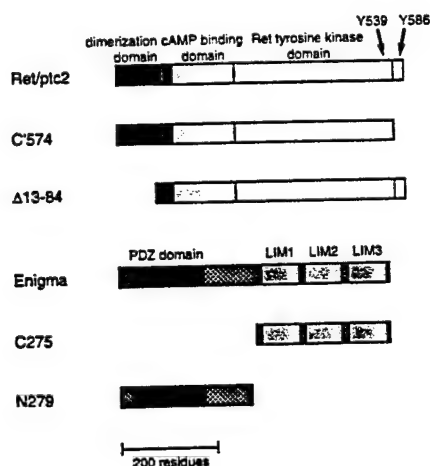


Figure 3. Ret/ptc2 is 596 residues in length, in which the N-terminal 236 amino acids are from the type I α regulatory subunit of cAMP dependent protein kinase (RI α) sequence. The dimerization domain of RI α is located between residues 12-62. Enigma is 455 residues in length, with an N-terminal PDZ domain and three C-terminal LIM domains. A hemagglutinin (HA) tag was added to the amino terminus of the Enigma constructs for detection by anti-HA monoclonal antibodies.

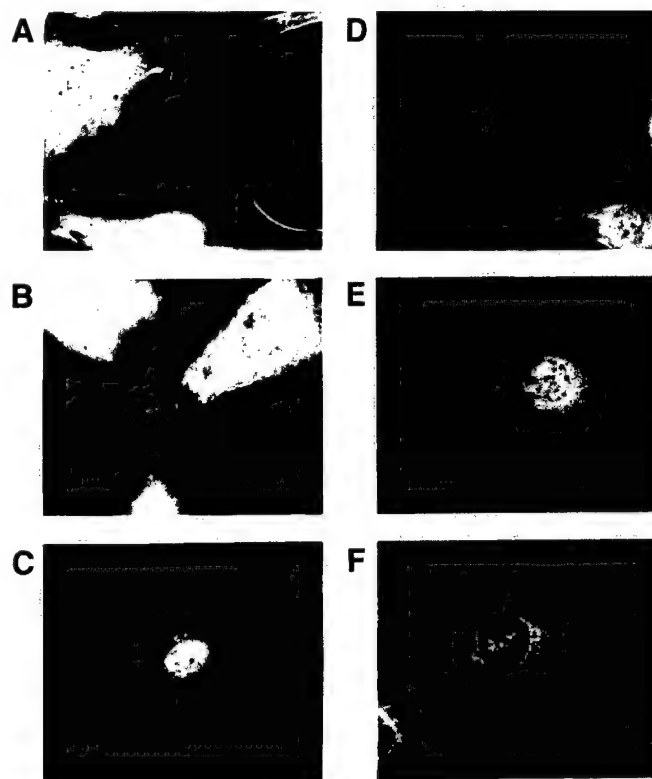


Figure 4. A- C: Sequence requirements for the sub-cellular targeting of Ret/ptc2. Fibroblasts microinjected with various Ret/ptc2 expression plasmids were fixed four hours after injection and immunofluorescently stained using anti-Ret antibodies. Constructs injected coded for: (A) wild-type Ret/ptc2, (B) Ret/ptc2-C'574, a mutant where the last 22 amino acids are missing, including the Enigma binding site, and (C) Ret/ptc2-D13-84, a dimerization domain deletion mutant. D-F: Sequence requirements for the sub-cellular targeting of Enigma. Cells injected with constructs expressing HA-tagged forms of Enigma were stained for immunofluorescence with anti-HA-tag monoclonal antibodies. Plasmids expressed the following HA-tagged protein: (D) full-length Enigma, (E) the C-terminal 275 residues of Enigma, which contain the three LIM domains, (F) the N-terminal 279 residues of Enigma, which contain the PDZ domain.

It was previously shown that Enigma interacts with the C-terminus of Ret/ptc2 via one of the C-terminal LIM domains of Enigma (34). These results raised the possibility that Enigma functions as an adapter protein with the N-terminal PDZ domain of Enigma anchoring an Enigma-Ret/ptc2 complex to a specific sub-cellular location. To test this possibility, cells were co-injected with plasmids expressing Ret/ptc2 and HA-tagged Enigma, and then co-stained for immunofluorescent confocal microscopy. The two proteins were found to co-distribute (Figure 5).

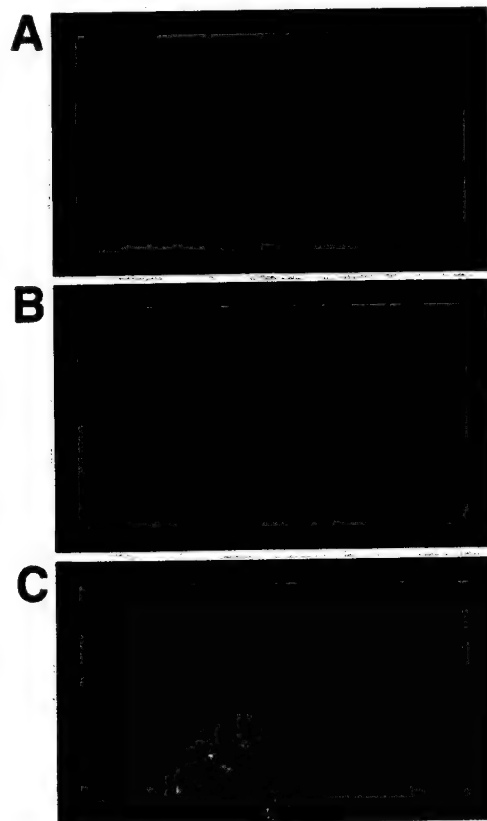


Figure 5. Mouse 10T1/2 fibroblasts co-injected with expression plasmids of Ret/ptc2 and HA-tagged Enigma were fixed four hours after injection, subjected to immunofluorescent staining, and then imaged by confocal microscopy. (A) Enigma distribution shown by fluorescein linked to anti-HA-tag monoclonal antibody. (B) Ret/ptc2 distribution shown by fluorescence of Cy-5 linked to anti-Ret antibody, (C) digital overlay of the two fluorescent signals.

Binding of Shc to Ret/ptc2 through its PTB domain

The adapter protein Shc binds to MEN2 mutant forms of RetR (49). Recently, other groups have found that both SH2 and PTB domains of Shc bind to RetR at Y1062 (50) and to Ret/ptc2 at Y586 (51). Because Shc recruits Grb2 to activated receptor tyrosine kinases, resulting in activation of the Ras-Raf pathway, the potential for Shc binding to Ret/ptc2 was investigated. Using a yeast two-hybrid approach, Shc was observed to bind to Ret/ptc2 in an interaction that was phosphorylation dependent because a catalytically inactive form of Ret/ptc2, K282R, failed to interact with Shc (Figure 6). The isolated PTB domain of Shc bound Ret/ptc2, while the SH2 domain alone did not. In addition, mutants of Ret/ptc2 which eliminated tyrosine 586 either by a point mutation (Y586F) or C-terminal truncation (C'574) failed to interact with Shc. These two-hybrid results were verified in stably transfected NIH3T3 cells which express the EGFR/Ret chimeric receptors, whereby stimulation by EGF results in activation of the Ret tyrosine kinase (38). Lysates of these cells were incubated with various GST fusion proteins bound to glutathione agarose. The phosphorylated chimeric receptor bound tightly to the GST-Shc PTB fusion, while no binding to the Shc SH2 domain was detected (Figure 6D). Binding of the EGFR/Ret chimera to Shc was ligand and autophosphorylation dependent whereas binding to the LIM2 domain of Enigma was not.

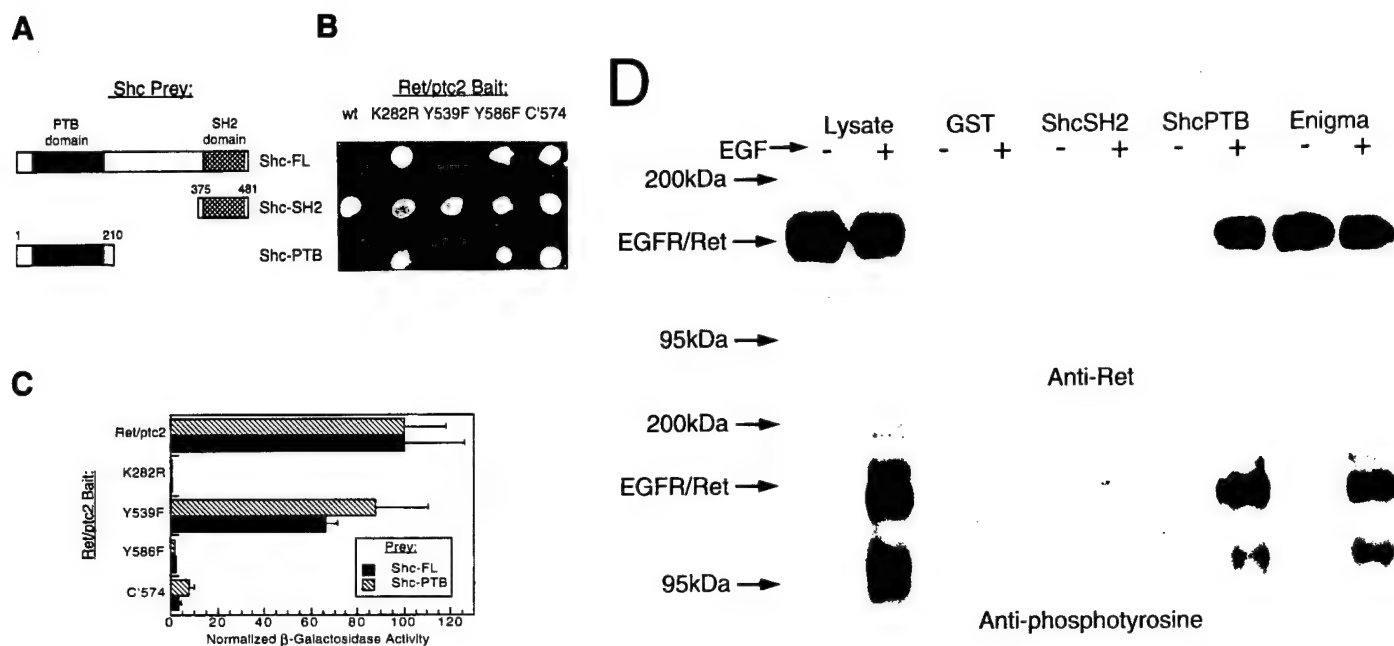


Figure 6. The yeast two-hybrid system was used to map the interaction determinants of Ret/ptc2 and Shc using various Shc-VP16 (Prey) and Ret/ptc2-LexA (Bait) fusion constructs, and results were verified by GST affinity precipitation. (A) Schematic representation of the Shc deletion mutants used where the numbers delineate amino acid sequences included in the constructs. (B) Qualitative β -galactosidase activity of yeast co-transformants. Single colonies were plated on solid media containing X-gal, and results shown are ten hours after plating. Bait constructs coded for wild-type Ret/ptc2, various point mutants, or a C-terminal truncation mutant (C'574). (C), Solution assay of yeast co-transformant β -galactosidase activity. Cultures of yeast co-transformed with plasmids expressing various Ret/ptc2-LexA and Shc-VP16 fusion proteins were assayed for β -galactosidase activity. Results shown are averages obtained for four assays with error bars representing the standard deviation. For comparison of results between the full-length and PTB Shc constructs, normalized values were plotted. Actual activity for full-length Shc with wild-type Ret/ptc2 was 250 Units, while the activity for the Shc PTB prey with wild-type Ret/ptc2 was 160 Units. Units are min^{-1} , as described in the text. (D) Clonal NIH3T3 cells expressing an EGFR/Ret chimeric receptor were treated (+) with or without (-) 100 nM EGF for 10 minutes at 37°C before lysis. Aliquots of lysates were incubated with either glutathione-S-transferase (GST) or GST-fusion proteins bound to glutathione agarose. The protein fragments expressed as GST fusions were the Shc SH2 and PTB domains, and second and third Enigma LIM domains. Western blots of EGFR/Ret that bound to the indicated GST fusion proteins are shown. Gels were run in parallel, blotted to PVDF membranes, and probed with anti-Ret (upper panel) or anti-phosphotyrosine antibodies (lower panel).

Use of chimeric proteins to elucidate the roles of Shc and Enigma

Both Shc and Enigma binding required tyrosine 586 of Ret/ptc2, a residue that is essential for mitogenic activity (32). We investigated whether either or both of these proteins were required for Ret-induced mitogenesis. The goal was to engineer a form of Ret/ptc2 that would bind Shc and not Enigma and another that would bind Enigma and not Shc. Because the consensus site for Shc PTB binding (52, 53, 54) closely resembles the consensus site for Enigma LIM interaction (34), a novel chimeric strategy was devised (Figure 7A). To test the importance of Enigma anchoring of Ret/ptc2, the "unanchored" C-terminal deletion form of Ret/ptc2, C'574, was fused to the N-terminal 279 residues of Enigma to make a chimeric protein referred to as C'574-PDZ. To engineer a form of Shc that would bind to Ret/ptc2 in the absence of tyrosine 586, PLC γ Shc was constructed in which the PTB domain of Shc was replaced with the N-terminal SH2 domain of phospholipase-C- γ (PLC γ). This SH2 domain of PLC γ interacts with tyrosine 539 of Ret/ptc2 (33, 55).

These chimeric proteins were first characterized in the two-hybrid system and then further characterized in transient transfections. Wild-type Shc interacted with Ret/ptc2, but failed to interact with any of the Ret/ptc2 forms lacking tyrosine 586, including the chimeric C'574-PDZ (Figure 7B, left panel). The PLC γ Shc chimeric adapter protein bound to all forms of Ret/ptc2 except the unphosphorylated, kinase-inactive K282R mutant (Figure 7B, right panel). This pattern of interaction was confirmed in mammalian cells when these same combinations of expression constructs were co-transfected into human embryonic kidney 293 cells.

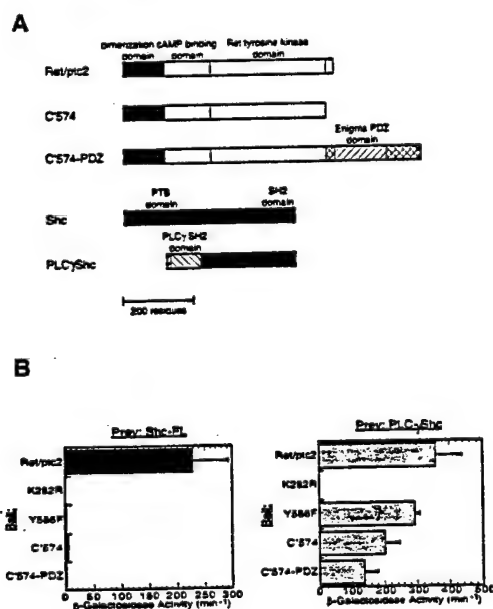


Figure 7. The yeast two-hybrid system was used to monitor interactions between various Ret/ptc2-LexA constructs and either Shc-VP16 or a PLC γ Shc-VP16 fusions. (A) Schematic representation of the fusion proteins constructed. A C-terminal 22 residue deletion mutant of Ret/ptc2 (C'574) was fused to the N-terminal 279 residues of Enigma to make C'574-PDZ. A fragment of PLC γ encoding the N-terminal SH2 domain was fused to the C-terminal two-thirds of Shc, replacing the Shc PTB domain (PLC γ Shc). (B), β -galactosidase activity of yeast co-transformed with the Ret/ptc2 and Shc constructs. Cultures of yeast co-transformed with plasmids expressing various Ret/ptc2-LexA and either Shc-VP16 or PLC γ Shc-VP16 fusion proteins were assayed for β -galactosidase activity. Results shown are averages of Units of activity from four solution assays with error bars representing the standard deviation.

Co-expression of Ret/*ptc2* with Shc resulted in Shc tyrosine phosphorylation, while Ret/*ptc2* constructs incapable of binding to Shc were also unable to phosphorylate Shc (Figure 8). In contrast, C'574 and C'574-PDZ were both able to phosphorylate PLC γ Shc.

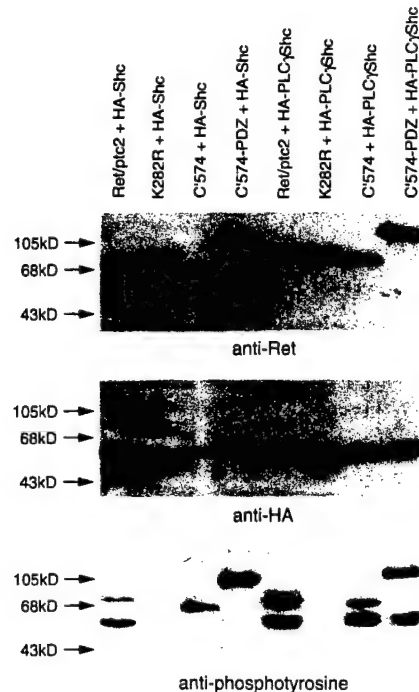


Figure 8. Human embryonic kidney 293 cells were co-transfected with plasmids expressing a form of Ret/*ptc2* and either HA-tagged Shc (HA-Shc) or PLC γ Shc (HA-PLC γ Shc). The Ret/*ptc2* constructs expressed wild-type Ret/*ptc2*, a kinase-inactive point mutant (K282R), a C-terminal truncation mutant (C'574), or a C-terminal replacement with the PDZ domain of Enigma (C'574-PDZ). Twenty-four hours after transfection, the cells were harvested, and lysates were separated by SDS-PAGE. Proteins were then transferred to PVDF membranes and detected with either anti-Ret (upper panel), anti-HA tag (middle panel), or anti-phosphotyrosine (lower panel) antibodies.

Rescue of the mitogenic activity of Ret/*ptc2*-C'574-PDZ, but not Ret/*ptc2*-C'574 by PLC γ Shc

To test which of the interactions are required for Ret/*ptc2* mitogenic signaling, the chimeric proteins were evaluated in the mitogenic microinjection assay. As shown previously (33), the C'574 mutant of Ret/*ptc2*, which does not bind to Enigma and Shc, was not mitogenically active (Figure 9). Adding the Enigma PDZ domain to make C'574-PDZ failed to increase mitogenic activity (Figure 9), despite the fact that this chimeric protein was sub-cellularly localized in the same distribution as that of Enigma and wild-type Ret/*ptc2* (data not shown). PLC γ Shc did not exhibit any mitogenic activity in this assay, and its

interaction with C'574 was not sufficient to rescue the mitogenic activity of this non-localized form of Ret/ptc2. Only co-expression of PLC γ Shc with C'574-PDZ resulted in significant stimulation of mitogenic activity (Figure 9).

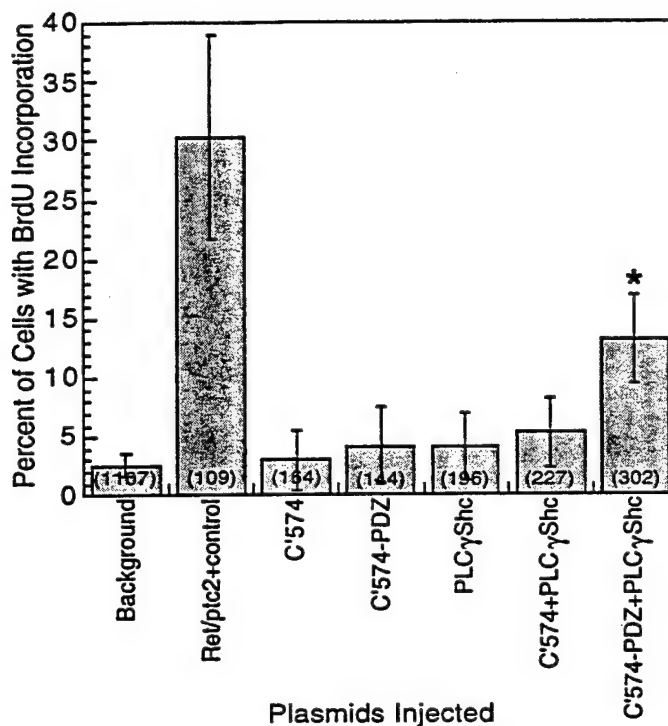


Figure 9. Serum-starved mouse 10T1/2 fibroblasts were microinjected with combinations of expression plasmids. In each case, constructs were injected at 100 μ g/ml, while background represents uninjected cells. Cells were then assessed for entry into S-phase by immunofluorescent detection BrdU incorporation. The fraction of injected cells positive for BrdU incorporation is shown with error bars displaying the 95% confidence interval calculated using the standard error of proportion. The numbers in parentheses are the total number of injected cells. The asterisk (*) denotes cells co-injected with plasmids for C'574-PDZ and PLC γ Shc were significantly above background in BrdU incorporation ($p < .001$).

Affinity precipitation of a Shc and Ret/ptc2 complex with GST-LIM2

To verify that a complex of Ret/ptc2 dimer binding to both Shc and Enigma was formed *in vivo*, affinity precipitation experiments were carried out using lysates from transfected 293 cells. The cells were co-transfected with constructs expressing HA-tagged Shc and either Ret/ptc2, or Ret/ptc2 D13-84. Both Ret/ptc2 and the form lacking the dimerization domain, Ret/ptc2 D13-84, bound to Enigma GST-LIM2 fusion protein (Figure 10, upper panel). However, Shc was only precipitated in the presence of dimeric, wild-type Ret/ptc2 (Figure 10, lower panel).

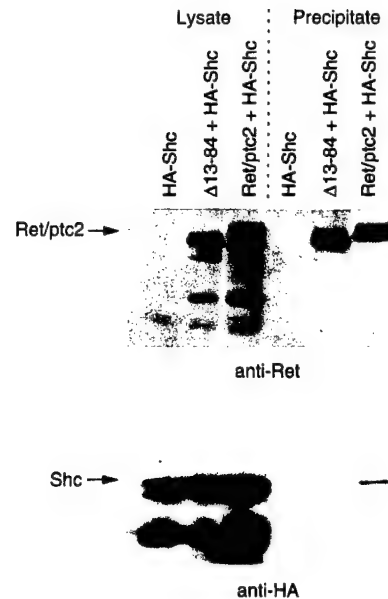


Figure 10. Lysates from 293 cells expressing HA-tagged Shc either alone, with wild-type Ret/ptc2, or Ret/ptc2 D13-84 were incubated with GST-LIM2 of Enigma bound to glutathione agarose. After extensive washing, the agarose beads were boiled in SDS sample buffer, and bound proteins were resolved by SDS-PAGE. Gels were run in parallel, blotted to PVDF membranes, and probed with anti-Ret (upper panel) or anti-HA antibodies (lower panel). Lysate samples, run in the first three lanes, were approximately one-fourth of the total amount of lysate used in each incubation.

This result demonstrates that a Ret/ptc2 dimer is capable of simultaneously binding to the LIM domain of Enigma and to Shc. We propose a model for Ret/ptc2 signaling through its dual association with Shc and Enigma (Figure 11).

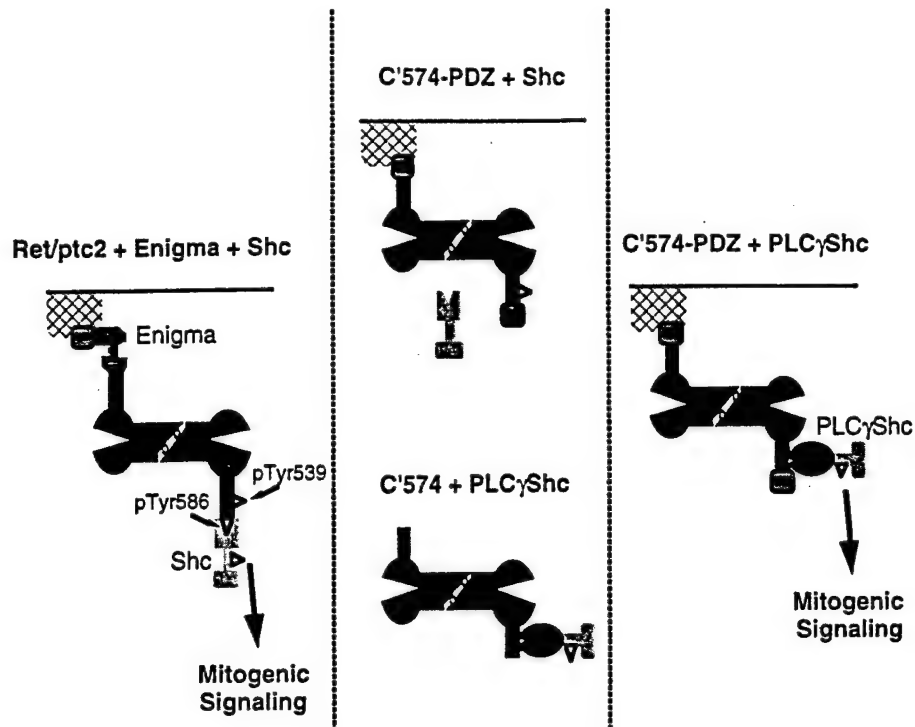


Figure 11. Proposed model for wild-type Ret/ptc2 mitogenic signaling.

B. Expression and Purification of His₆-Ret/ptc2

Although the expression of Ret/ptc2 in human embryonic kidney 293 cells, Sf9 insect cells, and *E. coli* was successful, the quantity of Ret/ptc2 produced in these expression systems was too low for quantitative purification, and extensive biochemical and biophysical characterization. Recently we attempted the expression of His₆-Ret/ptc2 in the wild-type strain, GS115 of the methylotrophic yeast, *Pichia pastoris*, in collaboration with Jim Hoeffler and Tom Purcell at Invitrogen (Carlsbad, CA). Small-scale expression preparations of either secreted or intracellularly expressed His₆-Ret/ptc2 were analyzed by SDS-PAGE and Western analysis using the anti-peptide Ret antibody. Intracellularly expressed His₆-Ret/ptc2 was overexpressed whereas the secreted protein was not detectable.

A typical coomassie stained 10% polyacrylamide gel of a 6 gm fermentor cell pellet preparation following lysis, metal chelate affinity chromatography, and peak fractions from anion exchange chromatography is shown (Figure 12). The corresponding chromatogram of the absorbance peaks, and both the linear NaCl and conductivity gradients from the Uno-Q1 (Bio-Rad) anion exchange chromatography separation is shown (Figure 13). The right arrowhead indicates the position of His₆-Ret/ptc2 (Figure 12, lanes 11 and 12) which is clearly purified from most of the other contaminating proteins (Figure 12, compare lanes 11 & 12 to lanes 4-10 and 13), and confirmed by Western analysis with the anti-Ret antibody (data not shown). The lower molecular weight bands present in the His₆-Ret/ptc2 purified from the Uno-Q1 column (Figure 12, lanes 11 and 12) are effectively removed via gel filtration in a Pharmacia preparative Superdex 200 column (data not shown). *P. pastoris* strain GS115 also produces a large amount of alcohol oxidase (74 kDa) (56) upon methanol induction of the alcohol oxidase promoter (Figure 12, lane 2 and 3). Alcohol oxidase migrates closely to the

monomer molecular weight of His₆-Ret/ptc2 but does not bind to the cobalt affinity resin as His₆-Ret/ptc2 (Figure 12, compare lanes 3 and 4). The last peak fraction of the chromatogram (Figure 13) did not stain with coomassie brilliant blue R-250 (Figure 12, lanes 14 and 15) and the high absorbance spike is characteristic for DNA. Typical yields of His₆-Ret/ptc2 are approximately 4-6 mg from a 6-8 gm frozen cell pellet.

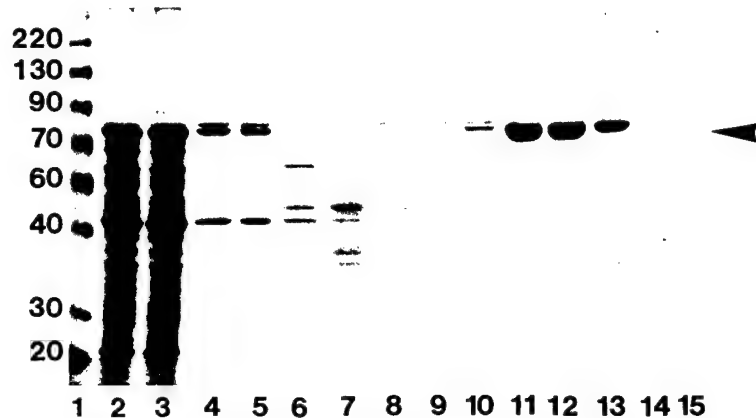


Figure 12. Coomassie stained SDS-PAGE of His₆-Ret/ptc2 purification from *P. pastoris* strain GS115. Lane 1: BRL Benchmark molecular weight standards, lane 2: S1 fraction, lane 3: S2 fraction unbound proteins, lane 4: pooled 10 mM imidazole elutions, lane 5: pooled 10 mM imidazole elutions after dialysis, centrifugation, and filtration, lane 6: BioLogic Uno-Q1 fraction 13, lane 7: fraction 14, lane 8: fraction 15, lane 9: fraction 16, lane 10: fraction 26, lane 11: fraction 27, lane 12: fraction 28, lane 13: fraction 29, lane 14: fraction 60, lane 15: fraction 61. The right arrow indicates the position of purified His₆-Ret/ptc2. Fractions 13-16 constitute fractions within Peak 1, fractions 26-29 are fractions within Peak 2 and fractions 60 & 61 are within Peak 3 in Figure 13.

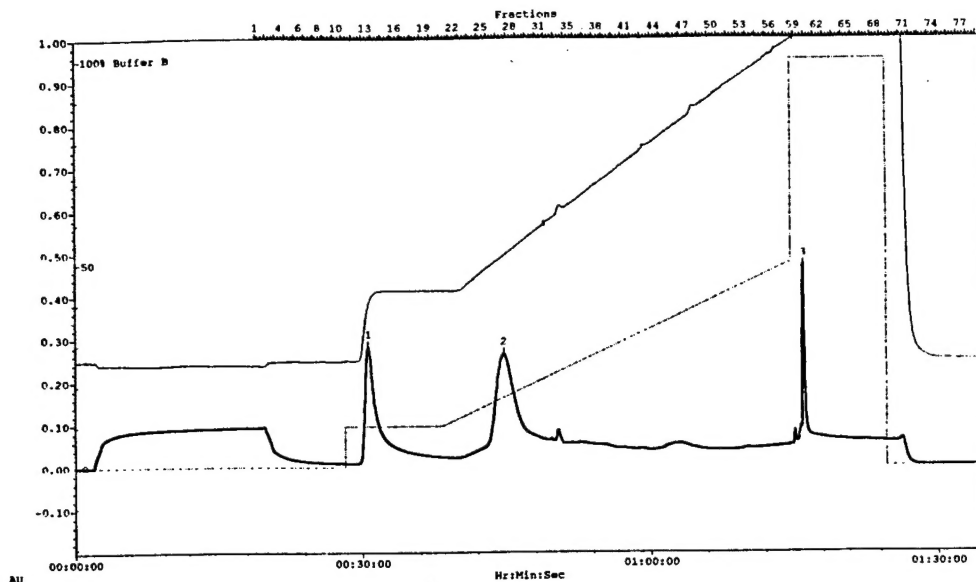


Figure 13. BioLogic Uno-Q1(Bio-Rad) anion exchange chromatogram of His₆-Ret/ptc2 at 1 ml/minute and 1.1% NaCl/minute. The absorbance peaks are numbered 1-3 and the NaCl and conductivity gradients are indicated. Buffer A: 20 mM Tris-Cl, pH 8, 100 mM NaCl, 5 mM β-mercaptoethanol, 5% glycerol. Buffer B: 20 mM Tris-Cl, pH 8, 1 M NaCl, 5 mM β-mercaptoethanol, 5% glycerol.

P. pastoris expressed His₆-Ret/ptc2 is active since it autophosphorylates in the presence of 10 mM MnCl₂ and [³²P]-dATP (Figure 14), and is stable at 4 °C in 50 mM HEPES, pH 8, 200 mM NaCl, 5% β-mercaptoethanol, 20% glycerol.



Figure 14. Autoradiography of [³²P]-dATP autophosphorylated His₆-Ret/ptc2 purified from *P. pastoris* and separated in a 10% SDS-PAGE gel reveals a single labeled band.

Preliminary *in vitro* [³²P]-dATP kinase assays indicate the effective concentration of His₆-Ret/ptc2 per 20 μl reaction is 300 pM (data not shown). Native gel electrophoresis yields a single His₆-Ret/ptc2 band (Figure 15, lane 1) that is larger than the 96 kDa cAPK R₂ dimer (Figure 15, lane 2), which indicates

the native solution form of active His₆-Ret/ptc2 is a single species that is larger than 96 kDa.



Figure 15. Native gel electrophoresis of *P. pastoris* purified His₆-Ret/ptc2 (lane 1) and the cAPK R₂ dimer (lane 2).

Isoelectric focusing of His₆-Ret/ptc2 revealed three isoforms that cluster about pI 6.55 (data not shown). The presence of at least 5 phosphorylated isoforms of His₆-Ret/ptc2 isolated from *E. coli* strain NovaBlue(DE3) was observed earlier in [³²P]-dATP autophosphorylation studies.

The molar absorptivity of His₆-Ret/ptc2 was calculated to be 156471 cm⁻¹M⁻¹. Absorbance measurements of the purified His₆-Ret/ptc2 revealed the absorption maxima is at 270 nm not 280 nm. Electrophoresis of the purified His₆-Ret/ptc2 in an ethidium bromide agarose gel revealed a high molecular weight DNA band. Future preparations of His₆-Ret/ptc2 will include DNaseI and 50 μM CaCl₂ in the lysis buffer to digest the contaminating chromosomal DNA. DNaseI can be easily removed at the anion exchange step of the purification since its pI is 11, and the oligonucleotides will be purified away from the protein at the final gel filtration step of the purification protocol.

Sedimentation equilibrium experiments of the presumably pure His₆-Ret/ptc2 confirmed the protein preparations contain a contaminant. Both absorbance and interference data sets at 7000, 10000 and 14000 xg predicted a protein mixture containing monomers, tetramers and octomers. The calculated molecular mass from the fitted data sets predicted a monomer molecular weight that was much larger than the theoretical monomer molecular weight of 70051 Da. The presence of contaminants in a protein sample can be detected in sedimentation velocity experiments but not in equilibrium experiments. Both the equilibrium and velocity experiments will be performed with purer protein preparations.

CONCLUSIONS

We have used a unique approach of employing chimeric forms of Ret/ptc2, Enigma and Shc to test whether Enigma localization or Shc interaction is important for Ret/ptc2 mitogenic signaling. Mutants of Ret/ptc2 in which the Shc docking site was absent were unable to phosphorylate Shc and mitogenically inactive. A deletion mutant of Ret/ptc2 that lacked an Enigma docking site was diffusely spread throughout the cytoplasm and also lacked mitogenic activity. When the Enigma docking site of Ret/ptc2 was replaced with the PDZ domain of Enigma, Ret/ptc2 was once again targeted to the cell edges, but this chimeric protein was unable to bind Shc and was mitogenically inactive. Mitogenic activity was restored only when this properly targeted form of Ret/ptc2 was co-expressed with the chimeric form of Shc, PLC γ Shc, a protein that is capable for interaction. These results indicate that both sub-cellular targeting of Ret/ptc2 by Enigma and interaction with phosphorylated Shc are required for Ret/ptc2 mitogenic signaling, and these results are summarized in the model (Figure 11).

The overexpression and purification of active, phosphorylated His₆-Ret/ptc2 in the yeast, *Pichia pastoris*, allows us to pursue a vigorous and comprehensive analyses of this unique oncogene. The results obtained so far are promising. Characterization of the biochemical and biophysical properties will provide further insights to our understanding of His₆-Ret/ptc2 at the molecular level.

REFERENCES

1. S. K. Hanks, T. Hunter, *Faseb J* **9**, 576-96 (1995).
2. S. S. Taylor, J. A. Buechler, W. Yonemoto, *Annu Rev Biochem* **59**, 971-1005 (1990).
3. D. R. Knighton, et al., *Science* **253**, 407-14 (1991).
4. S. S. Taylor, D. R. Knighton, J. Zheng, E. L. Ten, J. M. Sowadski, *Annu Rev Cell Biol* **8**, 429-62 (1992).
5. M. Takahashi, Y. Buma, M. Taniguchi, *Oncogene* **6**, 297-301 (1991).
6. V. Pachnis, B. Mankoo, F. Costantini, *Development* **119**, 1005-17 (1993).
7. A. Schuchardt, V. D'Agati, B. L. Larsson, F. Costantini, V. Pachnis, *Nature* **367**, 380-3 (1994).
8. R. Sugaya, S. Ishimaru, T. Hosoya, K. Saigo, Y. Emori, *Mech Dev* **45**, 139-45 (1994).
9. M. Trupp, et al., *Nature* **381**, 785-8 (1996).
10. S. Jing, et al., *Cell* **85**, 1113-24 (1996).
11. J. J. Treanor, et al., *Nature* **382**, 80-3 (1996).
12. P. Durbec, et al., *Nature* **381**, 789-93 (1996).
13. M. P. Sanchez, et al., *Nature* **382**, 70-3 (1996).
14. M. Takahashi, J. Ritz, G. M. Cooper, *Cell* **42**, 581-8 (1985).
15. Y. Ishizaka, et al., *Oncogene Res* **3**, 193-7 (1988).
16. T. Kunieda, M. Matsui, N. Nomura, R. Ishizaki, *Gene* **107**, 323-8 (1991).
17. L. M. Mulligan, et al., *Nature* **363**, 458-60 (1993).

18. R. M. Hofstra, et al., *Nature* **367**, 375-6 (1994).
19. L. M. Mulligan, et al., *Nat Genet* **6**, 70-4 (1994).
20. P. Edery, et al., *Nature* **367**, 378-80 (1994).
21. G. Romeo, et al., *Nature* **367**, 377-8 (1994).
22. M. Grieco, et al., *Cell* **60**, 557-63 (1990).
23. M. Grieco, et al., *Oncogene* **9**, 2531-5 (1994).
24. I. Bongarzone, et al., *Mol Cell Biol* **13**, 358-66 (1993).
25. I. Bongarzone, et al., *Cancer Res* **54**, 2979-85 (1994).
26. Q. Tong, et al., *Oncogene* **10**, 1781-1787 (1995).
27. F. Minoletti, et al., *Genes, Chromosomes & Cancer* **11**, 51-57 (1994).
28. M. Santoro, et al., *Oncogene* **9**, 509-16 (1994).
29. J. Bubis, T. S. Vedvick, S. S. Taylor, *J Biol Chem* **262**, 14961-6 (1987).
30. D. A. Leon, W. R. G. Dostmann, S. S. Taylor, *Biochemistry* **30**, 3035-40 (1991).
31. Y. Su, et al., *Science* **269**, 807-813 (1995).
32. K. Durick, et al., *J. Biol. Chem.* **270**, 24642-24645 (1995).
33. K. Durick, R. Y. Wu, G. N. Gill, S. S. Taylor, *J Biol Chem* **271**, 12691-4 (1996).
34. R. Wu, et al., *J Biol Chem* **271**, 15934-41 (1996).
35. T. A. Kunkel, K. Bebenek, J. McClary, *Methods Enzymol* **204**, 125-39 (1991).
36. A. B. Vojtek, S. M. Hollenberg, J. A. Cooper, *Cell* **74**, 205-14 (1993).
37. F. Ausubel, et al., *Current Protocols in Molecular Biology* (New York: Greene Publishing Associates and Wiley-Interscience), (1994).
38. M. Santoro, et al., *Mol Cell Biol* **14**, 663-75 (1994).
39. U. K. Laemmli, *Nature* **227**, 680-5 (1970).
40. M. Kozak, *Nucleic Acids Res* **15**, 8125-48 (1987).
41. M. Kozak, *Proc Natl Acad Sci U S A* **87**, 8301-5 (1990).
42. H. Cai, J. Szeberenyi, G. M. Cooper, *Mol Cell Biol* **10**, 5314-23 (1990).
43. L. A. Feig, G. M. Cooper, *Mol Cell Biol* **8**, 3235-43 (1988).
44. K. Pumiglia, et al., *Mol Cell Biol* **15**, 398-406 (1995).
45. S. E. Egan, et al., *Nature* **363**, 45-51 (1993).
46. E. J. Lowenstein, et al., *Cell* **70**, 431-42 (1992).
47. P. van der Geer, T. Hunter, R. A. Lindberg, *Annu. Rev. Cell Biol.* **10**, 251-337 (1994).
48. L.-S. Huang, K. Durick, J. Weiner, J. Chun, S. Taylor, *J Biol. Chem.* **272**, 8057-8064 (1997).
49. N. Asai, H. Murakami, T. Iwashita, M. Takahashi, *J Biol Chem* **271**, 17644-9 (1996).
50. M. J. Lorenzo, et al., *Oncogene* **14**, 763-71 (1997).
51. E. Arighi, et al., *Oncogene* **14**, 773-82 (1997).
52. T. A. Gustafson, W. He, A. Craparo, C. D. Schaub, T. J. O'Neill, *Mol Cell Biol* **15**, 2500-8 (1995).
53. A. A. Laminet, G. Apell, L. Conroy, W. M. Kavanaugh, *J Biol Chem* **271**, 264-9 (1996).
54. T. Trub, et al., *J Biol Chem* **270**, 18205-8 (1995).
55. M. G. Borrello, et al., *Mol Cell Biol* **16**, 2151-63 (1996).
56. P. Koutz, et al., *Yeast* **5**, 167-77 (1989).